Physica 17D (1985) 279–294
North-Holland, Amsterdam

LYAPUNOV NUMBERS AND THE LOCAL STRUCTURE OF ATTRACTORS

Edward N. LORENZ
Department of Earth, Atmospheric, and Planetary Sciences, Massachusetts Institute of Technology, Cambridge, Massachusetts 02139, USA

Received 10 September 1984

We examine an M-dimensional mapping defined by a system of broken linear equations, whose Lyapunov numbers may be prespecified, and whose directions of stretching and compression are the coordinate directions. With K positive and $M-K$ negative Lyapunov exponents, the attractor is locally the product of a K-dimensional continuum and an $(M-K)$-dimensional Cantor set; the latter is found to be a pseudo-product of Cantor sets or continua or Cantor sets and continua. When seen with finite resolution a pseudo-product may look like a true product, but its fractional dimension is less than the sum of the dimensions of its projections on the coordinate axes. Transitions in the number of Cantor sets and continua involved in the pseudo-product need not correspond to transitions in the integral part of the fractional dimension of the attractor. We speculate as to whether the attractors of continuous mappings and flows have similar structures.

1. Introduction

The numerous transformations which map the unit square or some other plane region into itself, and which possess strange or chaotic attractors, involve both stretchings and compressions. That is, certain pairs of points are mapped into more widely separated pairs, while other pairs become more closely spaced. A typical example is the Hénon mapping [1], which, after a linear transformation of Hénon's original variables, may be written

$$x_{n+1} = y_n,$$
$$y_{n+1} = bx_n - ay_n^2 + 1. \tag{1}$$

With $|b| < 1$, horizontally separated points are brought closer together, while vertically separated points are almost always moved farther apart. Hénon showed that with $b = 0.3$ and $a = 1.4$ a particular quadrilateral is mapped into itself.

Mappings in M dimensions may involve stretchings or compressions in several directions. For a flow, the Poincaré mapping defined by successive crossings of a specified hypersurface may involve similar stretchings and compressions.

Studies of the attractors of particular dynamical systems have frequently been accompanied by pictures of the attractor, or, if $M > 2$, of projections of the attractor on a plane. The standard procedure for producing such pictures consists of choosing a point at random and computing and plotting a long sequence of forward images. Often the leading points in the sequence, which may represent transient effects, are omitted. Sometimes the procedure is repeated with a second initial point to see whether a similar picture is obtained.

The literature contains a number of definitions of attractors, which are not all equivalent [2]. A definition which would appear to justify the pictorial procedure begins by defining a point Q as an attracting point (or limit point) for a point P if the sequence of forward images of P possesses a subsequence converging to Q. If the set of points P for which Q is an attracting point has Lebesgue measure exceeding zero, Q is a point of the attractor set A. Sometimes A is composed of a number of

disjoint sets with separate basins of attraction; each of these sets may then be called an attractor.

As pointed out by Ruelle [3], a computer-produced sequence of forward images is not a sequence of true images, because roundoff errors are introduced at each iteration. Ruelle has presented an alternative definition, which is aimed at reproducing the limiting form of a computer-produced attractor as the roundoff error approaches zero; he attributes some of the ideas to Conley [4].

Following Ruelle, but with different terminology, we define an ε-sequence of forward images as one where, before each iteration, the point to be mapped is displaced by a distance not exceeding a prechosen value ε. We define Q as an ε-attracting point of P if an ε-sequence originating at P possesses a subsequence converging to Q. We may then redefine Q as an attracting point for P if it is an ε-attracting point for P for arbitrarily small ε. We define A as before, but in terms of the redefined attracting points. An important effect of the new definition is to assure us, when it is not already assured, that the unstable manifold of any point Q of A – the set of points whose sequences of backward images asymptotically approach the sequence of backward images of Q – is contained in A.

Attractors can exhibit a wide variety of shapes, and it is to be expected that the complexity of these shapes will be related in some way to the relative amounts of stretching and compression. We can examine such a relationship quantitatively by invoking the familiar concepts of Lyapunov numbers and fractional dimension.

An infinitesimal M-dimensional sphere will be transformed by a mapping into an ellipsoid; continued iteration may produce a highly elongated and flattened ellipsoid. The factor by which the longest axis of the ellipsoid is multiplied during one iteration, averaged over many successive iterations, is the first Lyapunov number λ'_1; for the next to the longest axis it is the second Lyapunov number λ'_2, etc. The logarithms $l'_i = \log \lambda'_i$ are the Lyapunov exponents. For chaotic mappings of a region into itself, $l'_1 > 0$, while $l'_1 + \cdots + l'_M \leqq 0$.

Definitions of fractional dimension also involve multiplicative factors during one iteration of an operation, averaged over many iterations. Consider the number $N(\varepsilon)$ of M-dimensional cubes of side ε required to cover all points of a set. In general $N(\varepsilon)$ will increase as ε is reduced. If, when ε is repeatedly divided by ρ, where $\rho > 1$, the average factor by which $N(\varepsilon)$ is multiplied is ρ^d, the Hausdorff dimension or capacity [5] of the set is d. A set of real numbers for which $0 < d < 1$ is a Cantor set. The converse is not true; for some Cantor sets $d = 0$ or 1.

We may likewise consider the number $N'(\varepsilon)$ of cubes of side ε required to cover a fixed fraction, say one half, of the points of a set. If, on the average, $N'(\varepsilon)$ is multiplied by $\rho^{d'}$ when ε is divided by ρ, an alternatively defined fractional dimension is d'. In order to say what constitutes one half of the points of a set we must define some measure on the set. When the set is an attractor A, a natural measure of a subset is the fraction of the forward iterates of a point of A falling within the subset (the point chosen for iteration must avoid special points such as those whose sequences of iterates are periodic), and d' has been called the dimension of the natural measure [5], or the natural dimension. A suggested formula [6] for d', which is sometimes treated as an alternative definition, is

$$d' = L + \sum_{i=1}^{L} l'_i / |l'_{L+1}|, \tag{2}$$

where L is the largest integer making $l'_1 + \cdots + l'_L$ non-negative. In general $d' \leqq d$.

Particular systems where the complexity of A has been studied have tended to be confined to the minimum value of M for which $\Sigma l'_i$ may be negative while l'_1 is positive, i.e., $M = 2$ for a mapping or $M = 3$ for a flow (since a flow must have one vanishing Lyapunov exponent). This situation might be expected; a picture of the local structure of A should ideally show a cross section rather than a projection, and finding points which are on A and also on a given surface for a 3 dim-

ensional mapping, or on A and also on each of two given hypersurfaces for a 4-dimensional flow, can be an involved process.

Recently we sought the attractor of a 4-dimensional flow [7], whose equations are the four cyclic permutations of

$$dx_1/dt = c - x_1 + x_2(x_3 - x_4). \quad (3)$$

To obtain a 2-dimensional cross section we first determined a succession of points where an orbit intersected a chosen hyperplane. We then displaced each of these points slightly, along the manifold formed by the hyperplane and the local direction of maximum stretching, so that the orbit emanating from a displaced point would, several intersections later, simultaneously intersect the hyperplane and a second chosen hyperplane. Several successive approximations were generally needed to determine the proper displacement; convergence occurred about half of the time.

Fig. 1 shows one cross section, with $c = 100$. It appears to contain a Cantor set of curves, and the curves appear to be continua. We found that an arbitrary straight line cutting across the curves intersected A in a Cantor set, and concluded that locally the cross section was probably the product of a continuum and a Cantor set.

The Lyapunov exponents of the flow are 3.34, 0.00, −1.79, and −5.55, making $d' = 3.28$. With two negative exponents we had anticipated that the cross section might be locally the product of two Cantor sets, the sum of whose fractional dimensions would exceed unity.

For a 4-dimensional flow with $l_1' > 0$, but with $l_1' + l_2' + l_3' < 0$, we would anticipate that a cross section constructed in the manner of fig. 1 would contain no continua, since $d' < 3$; it will certainly possess no continua if $d < 3$. For more general dynamical systems we would expect that if the Lyapunov numbers vary more or less continuously as some parameter varies, transitions in the structure of A should occur. The purpose of the present study is to investigate such transitions for a suitable system, and to discover, if possible, what combinations of Lyapunov numbers correspond to these transitions.

In the following sections we shall first formulate a rather general class of dynamical systems. We shall then identify a subclass which is especially

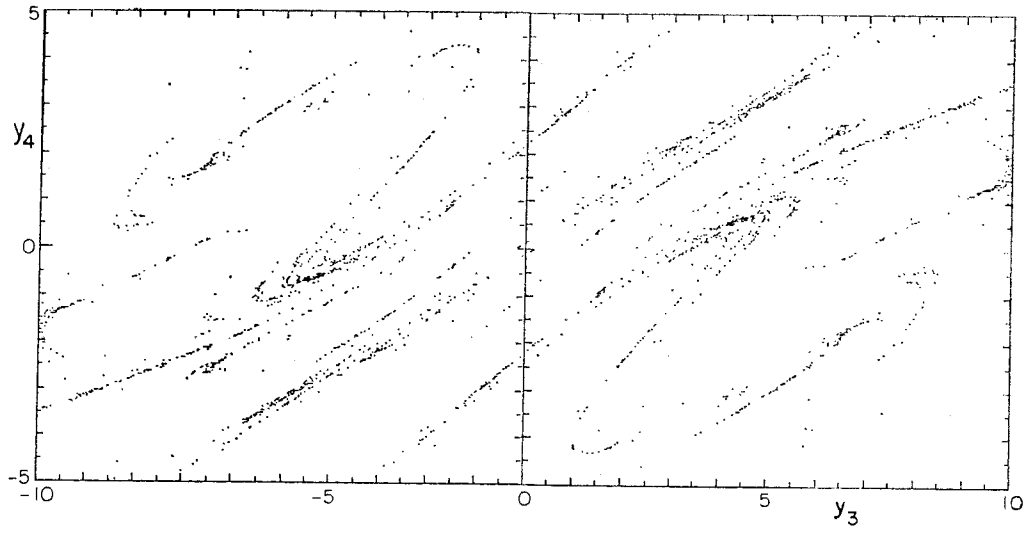

Fig. 1. A portion of the simultaneous intersection of the attractor of eq. (3), when $c = 100$, with the hyperplanes $x_1 + x_3 = 29$ and $x_2 + x_4 = -29$. The coordinates y_3 and y_4 are the orthogonal combinations $(x_1 + x_2 - x_3 - x_4)/2$ and $(x_1 - x_2 - x_3 + x_4)/2$ of the original coordinates.

suitable for our particular investigation. We shall see that there are indeed transitions in the structure of A, although they are not exactly like the ones which we had anticipated, and our results will suggest that the cross section in fig. 1 may be neither the product of a continuum and a Cantor set nor the product of two Cantor sets.

2. The equations

In our previous study [7] we noted that the system defined by eq. (3) acquires chaotic behavior, with $\lambda'_1 > 1$, when $c < -11.84$. We have subsequently found that the product $\lambda'_1\lambda'_2\lambda'_3$ (either $\lambda'_2 = 1$ or $\lambda'_3 = 1$) increases more or less continuously as c continues to decrease, passing unity near $c = -30$. Eq. (3) therefore appears to offer a suitable system for investigating transitions, and our original plan was to exploit this opportunity. We became discouraged when we found that the iterative procedure which converged about half of the time with $c = 100$ converged much less frequently with $c = -30$, and we subsequently elected to save one or two orders of magnitude of computation by investigating mappings instead of flows.

A fairly general class of mappings of the unit cube, where $0 \leqq x_i \leqq 1$ for $i = 1, \ldots, M$, into itself is given by

$$\begin{aligned} x_{i,n+1} &= x_{i+1,n}, \quad \text{if } i < M, \\ x_{M,n+1} &= cx_{1,n} + (1-c)F(x_{2,n}, \ldots, x_{M,n}), \end{aligned} \tag{4}$$

where $0 \leqq F(x_2, \ldots, x_M) \leqq 1$ throughout the unit cube, $0 < c < 1$, and $x_{i,n}$ is the nth iterate of an initial value $x_{i,0}$ of x_i. Eqs. (4) were modeled after the Hénon mapping of eqs. (1), and like that mapping may be rewritten as a uniquely invertible Mth order equation in a single variable. In general, points differing only in x_1 are brought closer together, while those with the same value of x_1 are carried farther apart. When $M = 2$ and F is a suitably chosen quadratic function, eqs. (4) become a special case of eqs. (1).

We are principally interested in mappings where $M \geqq 3$, where it may be possible to choose F so that variations of c, or of some parameter in the expression for F, will produce changes in the integral part of d'. Obvious candidates for F are polynomials and trigonometric functions. Fig. 2 shows the intersection of A with the plane $x_1 = 0$, obtained by a procedure analogous to the one used to produce fig. 1, when $M = 3$, $F(x_2, x_3) = \cos^2(\pi a x_2)$, $a = 2.6$, and $c = 0.75$. The Lyapunov exponents are approximately 0.15, -0.03, and -0.41, making d' about 2.3. As in fig. 1, there appears to be a Cantor set of curves, and the curves appear to be continua. Lower values of a, with $c = 0.75$, can make $d' < 2.0$.

The disadvantages of an investigation where c or F is varied systematically are that it may be hard to tell from inspecting a set of figures, or even from studying numerical output, just where a transition in the structure of A has occurred, while an exceedingly large number of iterations may be needed to stabilize the numerical estimates of the Lyapunov numbers. The results may therefore be rather inconclusive. Our final choice of a function F, which appears to circumvent these problems, follows the observation that a Poincaré mapping determined by a continuous flow may possess discontinuities. Among several orbits intersecting a

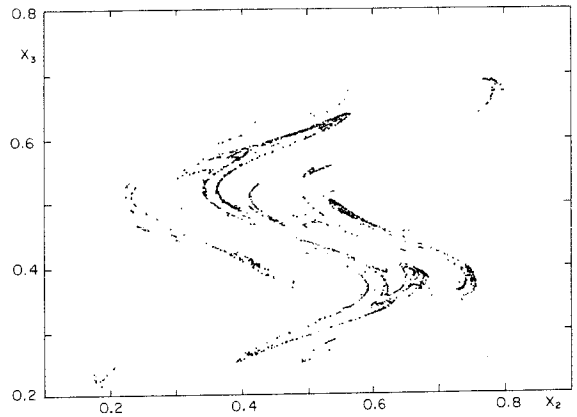

Fig. 2. The intersection of the attractor of eq. (4), when $M = 3$, $F(x_2, x_3) = \cos^2(\pi a x_2)$, $a = 2.6$, and $c = 0.75$, with the plane $x_1 = 0$.

specified hypersurface H at nearby points, one may prove to be tangent to H at a point P upon its next approach to H. Some neighboring orbits will then intersect H in points near P, while others will curve back and miss H altogether, eventually intersecting H much later at points far removed from P.

We shall therefore permit discontinuities in F. The simplest discontinuous functions would seem to be broken linear functions. Accordingly, we shall let

$$G(x_2,\ldots,x_M)=\sum_{i=2}^{M} a_i x_i, \tag{5}$$

and then let

$$F(x_2,\ldots,x_M)=G(x_2,\ldots,x_M)-J(x_2,\ldots,x_M), \tag{6}$$

where J is the largest integer not exceeding G. In matrix form eq. (4) then becomes

$$\begin{pmatrix} x_1 \\ \cdot\cdot \\ x_{M-1} \\ x_M \end{pmatrix}_{n+1} = \begin{pmatrix} 0 & 1 & \cdot\cdot & 0 \\ \cdot\cdot & \cdot\cdot & \cdot\cdot & \cdot\cdot \\ 0 & 0 & \cdot\cdot & 1 \\ c & (1-c)a_2 & \cdot\cdot & (1-c)a_M \end{pmatrix} \times \begin{pmatrix} x_1 \\ x_2 \\ \cdot\cdot \\ x_M \end{pmatrix}_n - \begin{pmatrix} 0 \\ \cdot\cdot \\ 0 \\ (1-c)J \end{pmatrix}_n, \tag{7}$$

or, with symbols for matrices,

$$\boldsymbol{X}_{n+1}=\mathbf{C}\boldsymbol{X}_n-\boldsymbol{J}'_n. \tag{8}$$

Since $\mathbf{C}$ is a matrix of constants, the Lyapunov numbers $\lambda'_1,\ldots,\lambda'_M$ are simply the absolute values of the eigenvalues $\lambda_1,\ldots,\lambda_M$ of $\mathbf{C}$. These satisfy the characteristic equation

$$\lambda^M-(1-c)\sum_{i=1}^{M-1} a_{i+1}\lambda^i-c=0. \tag{9}$$

We may therefore prespecify $\lambda_1,\ldots,\lambda_M$ and use eq. (9) to determine c and $a_2,\ldots,a_M$. In particular

$$c=-(-1)^M\prod_{i=1}^{M}\lambda_i. \tag{10}$$

Thus we may investigate the structure of A with no uncertainty as to the Lyapunov numbers. We shall restrict our attention to cases where $\lambda_1,\ldots,\lambda_M$ are real and distinct.

We may transform eq. (7) or (8) so that the directions of stretching and compression become the coordinate directions. If we let $\boldsymbol{Y}=\mathbf{DB}\boldsymbol{X}$ and $\boldsymbol{J}=-\mathbf{DB}\boldsymbol{J}'$, where $\mathbf{D}$ is a non-singular diagonal matrix, $\mathbf{B}$ is any matrix such that $\mathbf{BCB}^{-1}=\boldsymbol{\Lambda}$, and $\boldsymbol{\Lambda}$ is the diagonal matrix whose diagonal elements are $\lambda_1,\ldots,\lambda_M$ eq. (8) becomes

$$\boldsymbol{Y}_{n+1}=\boldsymbol{\Lambda}\boldsymbol{Y}_n+\boldsymbol{J}_n. \tag{11}$$

Evidently $\mathbf{B}$ is suitably chosen if the element in the ith row and jth column of $\mathbf{B}^{-1}$ is λ_j^{i-1}, whence the element in the ith row and final column of $\mathbf{B}$ is

$$b_{iM}=\prod_j(\lambda_i-\lambda_j)^{-1}, \tag{12}$$

where j runs over all values from 1 to M except i. Letting the ith diagonal element of $\mathbf{D}$ be $-(1-c)/b_{iM}$, we find that each element of $\boldsymbol{J}_n$ is simply J_n, and eq. (11) becomes

$$y_{i,n+1}=\lambda_i y_{i,n}+J_n. \tag{13}$$

Following some algebraic manipulation we find that

$$G_n=-\sum_{i=1}^{M}\left(\left(\lambda_i^{M-1}+(-1)^M\prod_j\lambda_j\right)\times\prod_j(\lambda_i-\lambda_j)^{-1}\lambda_i y_{i,n}\right), \tag{14}$$

each product running over all values of j except i, while J_n, which is the largest integer not exceeding G_n, is independent of i.

From eq. (13) it follows that

$$y_{i,n} = \lambda_i^{-1}(y_{i,n+1} - J_n). \tag{15}$$

If $y_{i,n+1} - J_n$ is substituted for $\lambda_i y_{i,n}$ in eq. (14), the terms containing J_n cancel, so that G_n and hence J_n are completely determined by $\boldsymbol{Y}_{n+1}$. Hence eq. (13), like the Hénon equation, is uniquely invertible.

Eq. (13) possesses certain advantages over eq. (7). In graphical work the preferred directions appearing in pictures of A or its projections should be the coordinate directions, and any other finding should alert us to some peculiarity. Fig. 3 shows a portion of the intersection of A with the plane $y_1 = -3$, when $M = 3$, $\lambda_1 = 1.5$, $\lambda_2 = -0.8$, and $\lambda_3 = -0.5$. The values of λ_i, which make $d' = 2.26$, were selected because the corresponding Lyapunov exponents are nearly proportional to those of fig. 1. Negative values for λ_2 and λ_3 were chosen because they produce smaller values of a_2 and a_3, and hence fewer discontinuities.

Again there appears to be a Cantor set of continua. The broken linearity has straightened out the curves, but otherwise the qualitative resemblance between the figures is good. Eq. (13) thus seems to define a suitable system for further study.

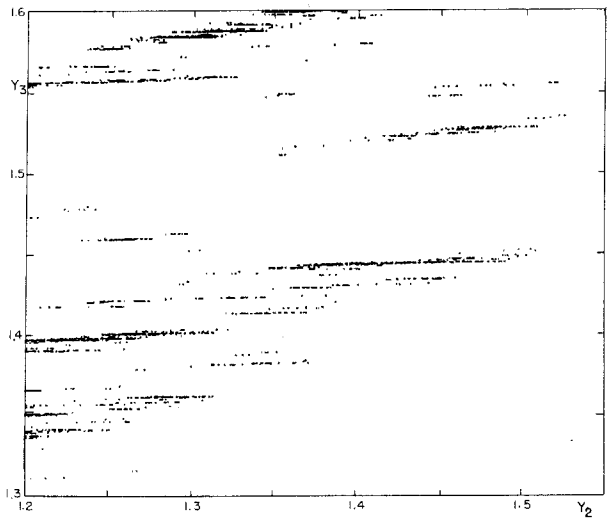

Fig. 3. A portion of the intersection of the attractor of eq. (13), when $M = 3$, $\lambda_1 = 1.5$, $\lambda_2 = -0.8$, and $\lambda_3 = -0.5$, with the plane $y_1 = -3$.

In analytical work eqs. (13) and (15) have the advantage of being solvable for $y_1, \ldots, y_M$ in terms of the sequence $\bar{J} = \{\ldots, J_{-1}, J_0, J_1, \ldots\}$ of integers. Assuming that no Lyapunov exponent vanishes, and letting K be the number of positive exponents, we find, since $y_{i,n}$ remains bounded as $n \to \infty$, that

$$\lambda_i y_{i,n} = -\sum_{j=0}^{\infty} \lambda_i^{-j} J_{n+j} \quad \text{when } i \leqq K, \tag{16}$$

while, for points on A, $y_{i,n}$ remains bounded as $n \to -\infty$, and

$$y_{i,n+1} = \sum_{j=0}^{\infty} \lambda_i^{j} J_{n-j} \quad \text{when } i > K. \tag{17}$$

The first K variables may therefore be expressed as power series with different arguments but with the same set of coefficients; the same is true for the remaining $M - K$ variables.

Thus each point on A may be identified with a unique sequence $\bar{J}$. Under this identification the mapping of eq. (13) becomes a subshift of finite type; these shifts have been studied in considerable detail, e.g. [8–11].

3. Some special sets

Before pursuing our primary task we shall examine some special sets of points whose coordinates are expressible as power series with integers as coefficients. Among these sets are the projections of the attractors of eq. (13) on the coordinate axes and, when $M > 2$, on certain coordinate planes or hyperplanes.

We first let $\bar{I} = \{\ldots, I_{-1}, I_0, I_1, \ldots\}$ be a two-way infinite sequence of integers containing a smallest and a largest integer. We shall call the one-way infinite sequences $\{\ldots, I_{-1}, I_0\}$ and $\{I_0, I_1, \ldots\}$ the past and the future halves of $\bar{I}$.

For $|\alpha| < 1$, we then define

$$r(\alpha, \bar{I}) = \sum_{k=0}^{\infty} I_k \alpha^k. \tag{18}$$

According to eqs. (16) and (17),

$$y_{i,0} = -\lambda_i^{-1} r\left(\lambda_i^{-1}, \bar{J}\right), \quad \text{when } i \leqq K, \tag{19}$$

while, for points on A, if $\bar{J}^*$ is the sequence $\{\ldots, J_1, J_0, J_{-1}, \ldots\}$ obtained by reversing the order of the integers in $\bar{J}$,

$$y_{i,1} = r(\lambda_i, \bar{J}^*), \quad \text{when } i > K. \tag{20}$$

We next let S be the ensemble of all sequences $\bar{I}$ satisfying a specified set of constraints on the integers which occur and on the order in which they occur. Different sequences in S may have identical past or future halves, and the constraints will specify what integers may immediately follow a given past half. We require that S be a stationary process; in particular, if $\bar{I}$ is in S, the sequences $\bar{I}'$ and $\bar{I}''$, with $I_n' = I_{n-1}$ and $I_n'' = I_{n+1}$, will be in S. Some of the consequences of constraints of this sort have been examined by Bowen and Lanford [12].

We then define $R_L(\alpha_1, \ldots, \alpha_L, S)$, as the set of all points $(x_1, \ldots, x_L)$ in L-dimensional space for which $x_i = r(\alpha_i, \bar{I})$ and $\bar{I}$ (independent of i) is in S. From eqs. (19) and (20) it follows that if S is the ensemble of all sequences $\bar{J}$ corresponding to points in A, and S^* is the ensemble of the related sequences $\bar{J}^*$, the projections of A on the $(y_1, \ldots, y_K)$- and $(y_{K+1}, \ldots, y_M)$-hyperplanes, aside from unequal linear compressions in the coordinate directions, are $R_K(\lambda_1^{-1}, \ldots, \lambda_K^{-1}, S)$ and $R_{M-K}(\lambda_{K+1}, \ldots, \lambda_M, S^*)$. More general sets R_L need not be associated with any attractor.

The simplest non-trivial allowable ensemble is the ensemble S_2 containing all sequences composed of 0's and 1's. Figs. 4, 5 and 6 show $R_2(\alpha, \beta, S_2)$ for different choices of α and β, as represented by 4000 randomly chosen points. Each set exhibits self-similarity; the lower and upper halves of each figure, corresponding respectively to the subensembles of sequences whose future halves begin with 0's and 1's, are superposable, and, aside from unequal compressions in the x- and y-directions (we write x, y for x_1, x_2), are copies of the complete figure. Likewise, the lower and upper halves of each half are copies of each half and of the complete figure, etc. The projections on the x- and y-axes are $R_1(\alpha, S_2)$ and $R_1(\beta, S_2)$.

If $\alpha < 1/2$, as in fig. 4, $R_1(\alpha, S_2)$ is a Cantor set. Each point of R_1 corresponds to exactly one

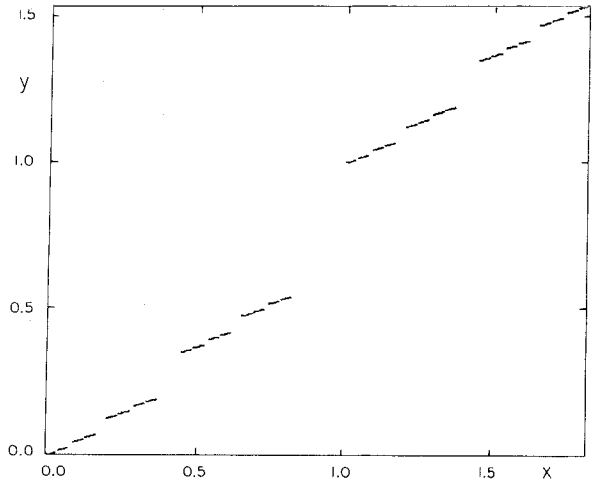

Fig. 4. The set $R_2(0.45, 0.35, S_2)$, where S_2 is the ensemble of all sequences of 0's and 1's. See text for definition of R_2.

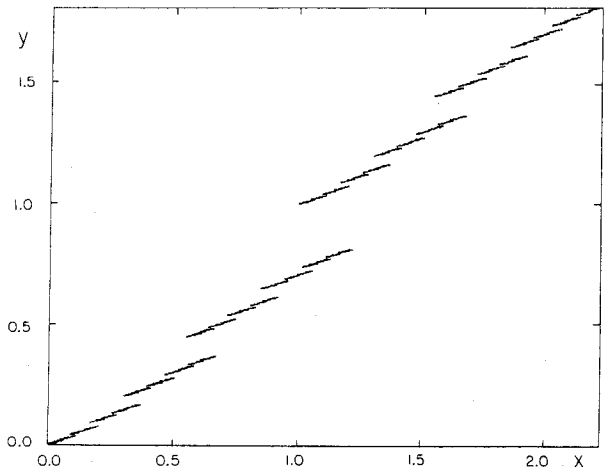

Fig. 5. Same as fig. 4, except set is $R_2(0.55, 0.45, S_2)$.

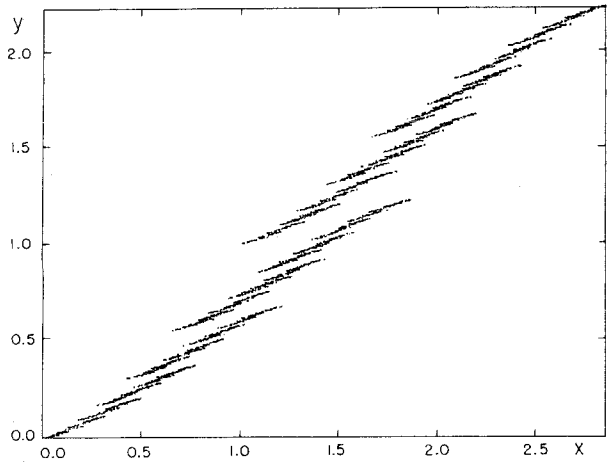

Fig. 6. Same as fig. 4, except set is $R_2(0.65, 0.55, S_2)$.

future half-sequence. If $\alpha = 1/m$ and m is an integer, the 0's and 1's in the future half of $\bar{I}$ are the successive digits in the expression for $r(\alpha, \bar{I})$ in base m, and R_1 is the set of numbers whose expressions in base M contain only 0's and 1's. If $\alpha = 1/3$, R_1 is the standard Cantor set obtained by removing middle thirds.

If $\alpha = 1/2$, $R_1(\alpha, S_2)$ is a continuum, and almost every point of R_1 corresponds to a single future half-sequence. Exceptions are rational fractions whose denominators are powers of 2, which correspond to two half-sequences. If $\alpha > 1/2$, as in figs. 5 and 6, $R_1(\alpha, S_2)$ is again a continuum, but now an uncountable number of future half-sequences $\bar{I}$ yield the same value of $r(\alpha, \bar{I})$. If $\alpha < 0$, $R_1(\alpha, S_2)$ and $R_1(-\alpha, S_2)$ are identical except for a translation.

Because of the self-similarity, 2^n segments of length $\alpha^n/(1-\alpha)$ will just cover $R_1(\alpha, S_2)$, if $\alpha \leqq 1/2$. Hence $d = \log 2/|\log \alpha|$. Obviously $d = 1$ when $\alpha \geqq 1/2$, while d is unchanged by changing the sign of α.

Analogous statements hold for the ensembles S_N containing all sequences composed of the N integers $0, \ldots, N-1$. More generally, $R_1(\alpha, S)$ is a Cantor set if α is sufficiently small, and a continuum if α is sufficiently large. We shall let $\sigma'(S)$ be the smallest value of α for which $r(\alpha, \bar{I})$ can assume the same value for two or more sequences $\bar{I}$ in S with distinct future halves, while $\sigma''(S)$ is the smallest value of α for which $R_1(\alpha, S)$ is a continuum. We shall also let $K_n(S)$ be the number of distinct sequences $\{I_0, \ldots, I_{n-1}\}$ of length n which can be subsequences of sequences $\bar{I}$ in S, while $\rho(S)$ is the limiting value of K_{n+1}/K_n as $n \to \infty$. Obviously $\rho(S_N) = N$, while $\sigma'(S_N) = \sigma''(S_N) = 1/N$. We shall call an ensemble S for which $\sigma' = \sigma'' = 1/\rho$ *well-behaved*, regardless of whether $S = S_N$ for any N; otherwise it is *ill-behaved*.

Some simple examples where $S \neq S_N$ are the ensembles of all sequences of 0's and 1's which do not contain two 1's in succession, and of all sequences of 0's and 1's which never contain fewer than three 0's in succession. Fig. 7 contains branching diagrams for these ensembles, showing all sequences of six terms or fewer which can be

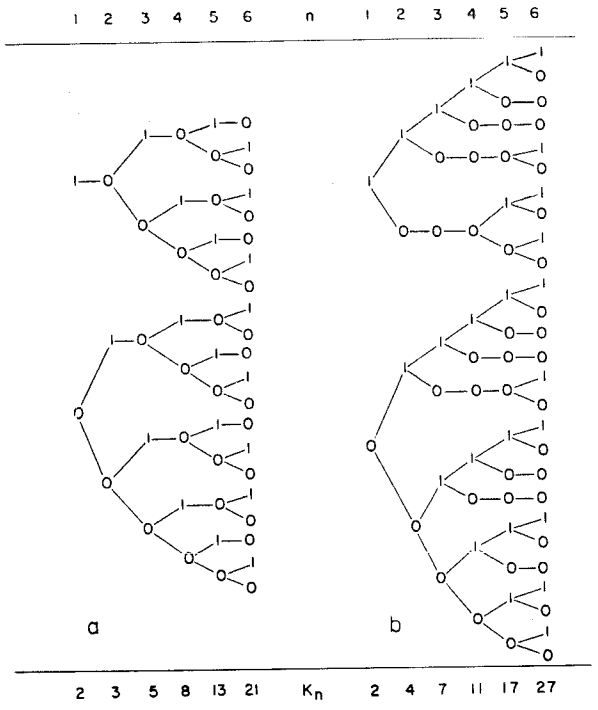

Fig. 7. A branching diagram showing all subsequences, with 6 terms or fewer, of sequences of 0's and 1's where two or more 1's in succession cannot occur. (b) Same as (a), for sequences of 0's and 1's where fewer than three 0's in succession cannot occur.

subsequences of sequences in S. Values of n and K_n are tabulated.

In fig. 7a, which pertains to the first example, each column is identical to the column which would be formed by placing the column immediately to the left below the next column to the left. Hence $K_n = K_{n-1} + K_{n-2}$, and $\rho(S)$ is the Fibonacci ratio 1.618 satisfying the equation $\rho^2 - \rho - 1 = 0$. We observe also that all branchings in fig. 7a are identical; the future half-sequence immediately below each branching is $0,1,0,1,\ldots$, while the one immediately above is $1,0,0,0,\ldots$. These yield equal values of $r(\alpha, \bar{I})$ if $\alpha/(1-\alpha^2) = 1$, or $\alpha = 0.618 = 1/\rho$. Hence $\sigma' = \sigma'' = 0.618$, and S is well-behaved.

In fig. 7b, pertaining to the second example, we find that $K_n = K_{n-1} + K_{n-4} + (K_{n-1} - K_{n-2})$, so that ρ is again the Fibonacci ratio 1.618 satisfying the factorable equation $\rho^4 - 2\rho^3 + \rho^2 - 1 = 0$. However, the branchings are not identical. The sequences immediately below and above a 0-branching are $0,1,1,1,\ldots$ and $1,0,0,0,\ldots$, which yield equal values of $r(\alpha, \bar{I})$ if $\alpha/(1-\alpha) = 1$, or $\alpha = 1/2$, while the sequences immediately below and above a 1-branching are $0,0,0,1,1,\ldots$ and $1,0,0,0,0,\ldots$ which yield equal values of $r(\alpha, \bar{I})$ if $\alpha^3/(1-\alpha) = 1$, or $\alpha = 0.682$. Thus $\sigma' = 0.500$, $1/\rho = 0.618$, and $\sigma'' = 0.682$, and S is ill-behaved.

Returning to fig. 4, where S is well-behaved and $\beta < \alpha < 1/\rho$, we see that each value of x corresponds to a single sequence $\bar{I}$, which determines a single value of y, and vice versa. The ρ^n segments of length $\alpha^n/(1-\alpha)$ which cover $R_1(\alpha, S)$ can, if replaced by squares of side $a^n/(1-\alpha)$, be displaced vertically to cover $R_2(\alpha, \beta, S)$, so that R_2 and R_1 have the same capacity. It follows that R_2 is not the product of its projections $R_1(\alpha, S)$ and $R_1(\beta, S)$, which would have a higher capacity, and it is not obviously the product of any other Cantor sets. It is more like a one-dimensional Cantor set lying on a distorted line. We shall call the Cantor set $R_2(\alpha, \beta, S)$ a *pseudo-product* of the Cantor sets $R_1(\alpha, S)$ and $R_1(\beta, S)$.

When $\beta < 1/\rho < \alpha$, as in fig. 5, each value of y determines one value of x, but each value of x determines a Cantor set of values of y. Since $R_2(\alpha, \beta, S)$ may, if compressed to fit the unit square, be covered by ρ^n rectangles of vertical width β^n, each of which may be covered by $(\alpha/\beta)^n$ squares of side β^n, $d = 1 + \log(\rho\alpha)/|\log\beta|$. Again R_2 is not the product of its projections, since again its capacity is too small. It might be called a continuum of Cantor sets, since a one-dimensional Cantor set of capacity $\log(\rho\alpha)/|\log\beta|$ lies above each point on the x-axis. It is certainly not a Cantor set of continua, since it contains no continua; the obvious gaps between the halves, quarters, etc., of fig. 5 are accompanied by unresolved gaps which separate any pair of points. We shall call $R_2(\alpha, \beta, S)$ a pseudo-product of the continuum $R_1(\alpha, S)$ and the Cantor set $R_1(\beta, S)$.

When $\alpha\beta < 1/\rho < \beta < \alpha$, as in fig. 6, there are again gaps between any two points, even though both projections are continua. Here we shall call $R_2(\alpha, \beta, S)$ a pseudo-product of the two continua. Again $d = 1 + \log(\rho\alpha)/|\log\beta|$. Only when $\alpha\beta \geqq 1/\rho$ does R_2 become a true two-dimensional continuum, with $d = 2$.

The sets in figs. 4–6 are all concentrated near the diagonal line $(1-\alpha)x = (1-\beta)y$, since α/β is close to unity. We can avoid this outcome by letting α and β have opposite signs. Fig. 8 shows $R_2(0.55, -0.45, S_2)$. Its projections are identical to those in fig. 5, except for a translation, and it is again a pseudo-product of a continuum and a Cantor set, but it looks more like a true product of diagonally oriented Cantor sets.

We can also let α/β be large. Fig. 9 shows the left-hand half of $R_2(0.75, 0.25, S_2)$. Again it is a pseudo-product of a continuum and a Cantor set, but it could easily be mistaken for a true product. Since $0.25 = (0.75)^5$ approximately, points on the same horizontal segment differing by $1/4$ unit in x differ by only $1/1000$ units in y, which is visually undetectable. Points differing by 10^{-4} units in x differ by only 10^{-20} units in y, which would not be revealed by a typical double-precision numerical printout. The horizontal projection of an arbitrarily narrow horizontal strip which intersects the

set is a continuum, and any vertical line passing between the horizontal extremities of the set intersects the set in a Cantor set. Only a knowledge of how the set is defined reveals that a *horizontal* strip of finite width passes between any two points of the set.

Although figs. 5 and 8, when viewed globally, do not appear vulnerable to a similar misinterpretation, it should be remembered that a sufficiently small piece of either figure, when sufficiently magnified, looks like the complete figure, except that it is highly compressed in the vertical direction. On a sufficiently local scale, then, the pseudo-products in figs. 5 and 8 look much like fig. 9, and could be mistaken for true products.

Similar considerations apply when $S = S_N$ for $N > 2$, or when $S \neq S_N$ for any N. Fig. 10 shows $R_2(0.45, 0.35, S_3)$. It is a pseudo-product of two continua, and looks much like fig. 6 except that thirds instead of halves are superposable. Fig. 11

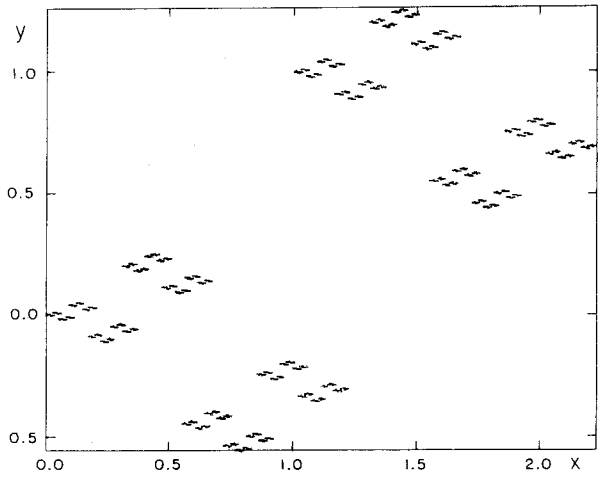

Fig. 8. Same as fig. 4, except set is $R_2(0.55, -0.45, S_2)$.

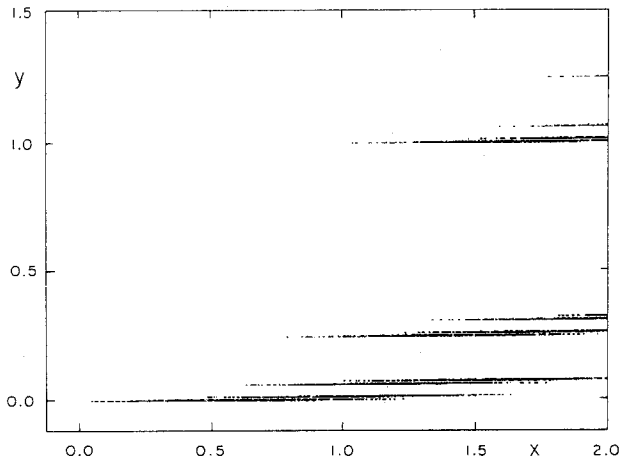

Fig. 9. Same as fig. 4, except set is $R_2(0.75, 0.25, S_2)$, and only the left-hand half is shown. The right-hand half may be obtained by rotating the left-hand half through 180° about the point $(2, 2/3)$.

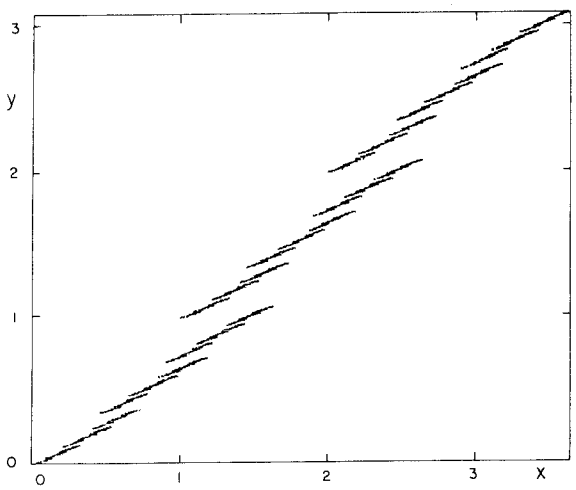

Fig. 10. Same as fig. 4, except set is $R_2(0.45, 0.35, S_3)$, and S_3 is the ensemble of all sequences of 0's, 1's and 2's.

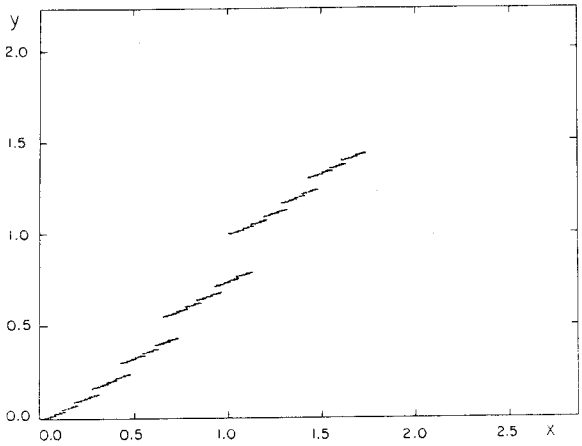

Fig. 11. Same as fig. 4, except set is $R_2(0.65, 0.55, S)$, and S is the ensemble of all sequences of 0's and 1's where two or more 1's in succession cannot occur.

shows $R_2(0.65, 0.55, S)$ for the well-behaved ensemble S whose branching diagram appears in fig. 7a. It is a subset of the set in fig. 6, but, since $\rho(S) = 0.618$, it is a pseudo-product of a continuum and a Cantor set, locally resembling fig. 5.

When S is ill-behaved, R_2 may acquire a more complicated structure. Fig. 12 shows $R_2(0.65, 0.55, S)$ for the ensemble S whose branching diagram appears in fig. 7b. Since $\sigma' < \beta < 1/\rho < \alpha < \sigma''$, R_2 must be considered a pseudo-product of Cantor sets, but it does not resemble the pseudo-product shown in fig. 4; each value of y corresponds to many values of x, and vice versa. In particular, the projection $R_1(\alpha, S)$ is a Cantor set of capacity 1, whose left-hand portion could easily be mistaken for a continuum.

More generally, a Cantor set $R_L(\alpha_1, \ldots, \alpha_L, S)$ may be a pseudo-product of K continua and $L - K$ one-dimensional Cantor sets. If $|\alpha_k| < 1/\rho(S)$, or, for an ill-behaved ensemble, if $|\alpha_k| < \sigma'(S)$, the value of x_k uniquely determines the values of the other coordinates of any point. When compressed into the unit square, R_L may be covered by ρ^n cubes of side α_1^n, or by ρ^n boxes of thickness α_2^n, each of which may be covered by $(\alpha_1/\alpha_2)^n$ cubes of side α_2^n, or by ρ^n boxes of width α_3^n, each of which may be covered by $(\alpha_1\alpha_2/\alpha_3^2)^n$ cubes of diameter α_3^n, etc. The capacity d is therefore the minimum of $d_0, \ldots, d_L$, where, if for conciseness we set $\alpha_0 = \rho$ and $\alpha_{L+1} = 0$,

$$d_k = k + \log(\alpha_0 \cdots \alpha_k)/|\log \alpha_{k+1}|. \tag{21}$$

Evidently $d_{k-1} = d_k = k$ when $\alpha_0 \cdots \alpha_k = 1$; otherwise d_k is minimized when k is the largest integer making $\alpha_0 \cdots \alpha_k > 1$.

Thus, if $\alpha_1, \ldots, \alpha_L$ are continuously varied, while S remains well-behaved, the integral part of d changes when $\alpha_1 \cdots \alpha_k = 1/\rho$ for some k, while the number of coordinate axes on which the projections of R_L are continua rather than Cantor sets changes when $\alpha_k = 1/\rho$ for some k. If S is ill-behaved, the latter changes occur when $\alpha_k = \sigma''(S)$.

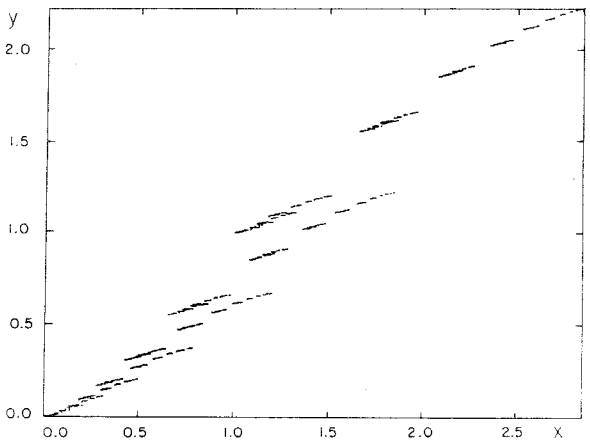

Fig. 12. Same as fig. 4, except set is $R_2(0.65, 0.55, S)$, and S is the ensemble of all sequences of 0's and 1's where fewer than three 0's in succession cannot occur.

4. Two-dimensional mappings

Mappings with $M = 2$ share many properties with higher-dimensional mappings, in which we are mainly interested. With $M = 2$, eq. (13) may be written

$$\begin{aligned} x_{n+1} &= \lambda_1 x_n + J_n, \\ y_{n+1} &= \lambda_2 y_n + J_n, \end{aligned} \tag{22}$$

where J_n is the largest integer not exceeding G_n, and

$$(\lambda_1 - \lambda_2)G_n = -(\lambda_1 + \lambda_2)(\lambda_1 x_n - \lambda_2 y_n). \tag{23}$$

Somewhat similar broken linear mappings include the "skinny baker's transformation" of Alexander and Yorke [13]; this is a special case of the generalized baker's transformation analyzed in detail by Farmer et al. [5].

Fig. 13 shows A when $\lambda_1 = 4/3$ and $\lambda_2 = -1/3$. It was constructed by plotting 4000 successive iterates of a particular point, after discarding the first 1000 iterates as possibly representing transient effects. We assume that A is defined in such a way that the unstable manifold of each point in A is contained in A.

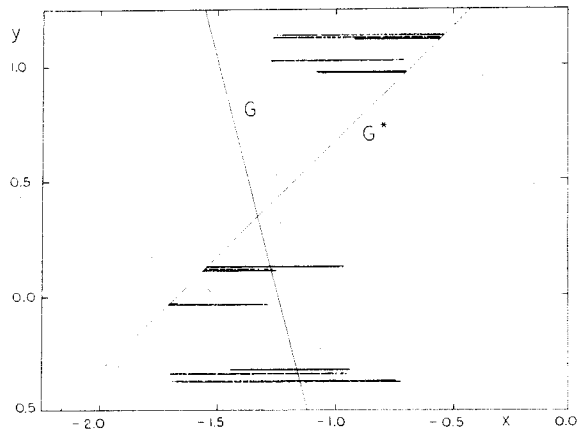

Fig. 13. The attractor of eq. (13), when $M = 2$, $\lambda_1 = 4/3$ and $\lambda_2 = -1/3$. The line G is the line where $G(x, y) = 1$. The line G* is the forward image of G.

The sloping line labeled G is the line $4x + y + 5 = 0$, where $G = 1$, while the line G^* is its forward image $3x - 3y + 5 = 0$. The line $G = 2$ does not intersect A, so that values of J_n are confined to 0's and 1's. Points to the right or left of G, where $J = 0$ or 1 respectively, are mapped into points to the right or left of G*.

Superficially the local structure in fig. 13 resembles that in fig. 9, but actually the coordinates of a point in fig. 9 are $r(\alpha, \bar{I})$ and $r(\beta, \bar{I})$, for the same sequence $\bar{I}$, while in fig. 13 they are $r(1/\lambda_1, \bar{J})$ and $r(\lambda_2, \bar{J}^*)$, for two different even though related sequences $\bar{J}$ and $\bar{J}^*$. There is thus no need for a value of y to determine a unique value of x, as it does in fig. 9, and hence no need for A to be a pseudo-product. Indeed, we would expect A to be the true product of a continuum and a Cantor set [8, 14].

To see what constraints have been placed on the ensemble S of sequences $\bar{J}$, we may examine a long sequence of 1's and 0's. We shall represent the sequence symbolically by a succession of pairs of numbers; the members of a pair indicate a number of successive 0's and a subsequent number of successive 1's. For example, the subsequence 0, 0, 0, 1, 0, 1, 1, 0, 0, 1, 1, 1, if preceded by 1 and followed by 0, would be coded as 31 12 23.

Fig. 14a shows 400 successive pairs in a particular solution. The most obvious features are that the second member of a pair is always 1, indicating that, as in fig. 7a, a sequence cannot contain two successive 1's, while the first member is always 1, 2, or 3, indicating that a sequence cannot have more than three successive 0's.

If these were the only constraints, a branching diagram like fig. 7a or 7b would show that $\rho = 1.47$. Actually there are further constraints; for example, two "31" pairs do not occur in succession. Hence $\rho < 1.47$. It would be difficult to identify all of the constraints, some of which involve long subsequences, but fortunately it is not necessary.

Consider the succession of backward or inverse images of a horizontal segment of length ε

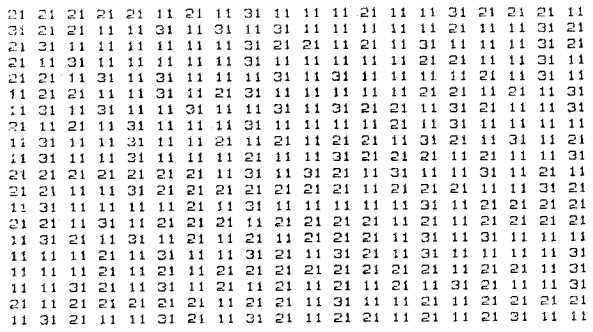

a

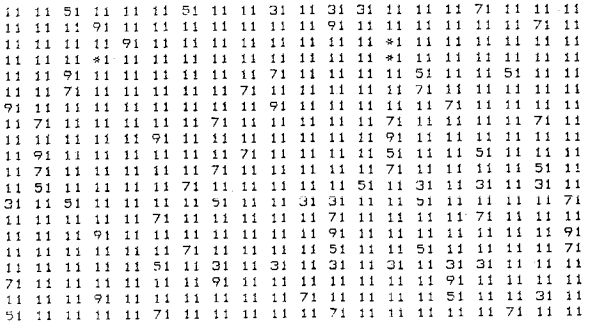

b

Fig. 14. (a) Symbolic representation of a particular sequence of 0's and 1's generated by eq. (13), when $M = 2$, $\lambda_1 = 4/3$ and $\lambda_2 = -1/3$. See text for explanation of symbolic representation. (b) Same as (a), except $\lambda_1 = 1.0145$ and $\lambda_2 = -0.9465$.

containing a randomly chosen point P in A. The nth inverse image will be a segment of length ε/λ_1^n, unless one of the previous inverse images intersects G*. It is to be expected that P will possess inverse images arbitrarily close to G*, but, since the images of the segment decrease exponentially in length, there is a positive probability that no image will intersect G*; this probability is high if ε is small. The inverse images of the segment thus approach those of P asymptotically, i.e., the discontinuity in the mapping does not prevent the unstable manifold of P, and hence the set A, from containing a segment which contains P.

Points on a horizontal segment correspond to sequences in S with identical past halves and different future halves. Since a point (x, y) determines a sequence, two different sequences yielding the same value of y cannot yield the same value of x, i.e., $r(1/\lambda_1, \bar{J})$ cannot assume the same value for two different future half-sequences $\bar{J}$, and $1/\lambda_1 \leqq \sigma'(S)$. Since the sequences yielding the same value of y together yield a continuum of points, $1/\lambda_1 \geqq \sigma''(S)$. Since by definition $\sigma' \leqq \sigma''$, it follows that $\sigma' = \sigma'' = 1/\lambda_1$.

Consider next the succession of forward images of a horizontal segment of length ε containing P. At each iteration those segments intersecting G will split into two segments; these splits correspond to branchings in a diagram like fig. 7a or 7b. The nth image will be a number of segments whose combined length is $\lambda_1^n\varepsilon$. As $n \to \infty$, the number of segments will increase as ρ^n, so that the average length will vary as $(\lambda_1/\rho)^n$. Certainly the average length cannot exceed the diameter of A; neither can it become too small, since then most of the segments would not intersect G, and the average length would increase upon the next iteration. Hence the average length remains comparable to the diameter of A, and $\rho(S) = \lambda_1$. Combining our results, we see that $\sigma' = \sigma'' = 1/\rho$, and we conclude that S is well-behaved.

Although the sequences in S^* need not be those in S, the number $K_n(S^*)$ of subsequences of length n certainly equals $K_n(S)$, since the subsequences in S^* are simply the reversed subsequences in S. Whether or not S^* is well-behaved, we conclude that $\rho(S^*) = \lambda_1$.

Since $|\lambda_2| < 1/\lambda_1$, the projection $R_1(\lambda_2, S^*)$ of A on the y-axis must be a Cantor set. Locally, then, A may be considered the product of the continuum $R_1(1/\lambda_1, S)$ and a Cantor set. We must recognize, however, that among the horizontal segments contained in A and penetrating any small square, a few will terminate inside the square. The smaller the square, the larger the fraction of segments which pass completely through it.

Since $\rho = \lambda_1$, the capacity of $R_1(\lambda_2, S^*)$ is $\log \lambda_1'/|\log \lambda_2'|$, so that the capacity of A is $1 + \log \lambda_1'/|\log \lambda_2'|$. Comparing eq. (2), we see that $d' = d$. For fig. 13, $d = \log_3 4 = 1.26$.

Other choices of λ_1 and λ_2 may produce differently shaped attractors. Fig. 15 shows one half of the attractor set when $\lambda_1 = 1.0145$ and $\lambda_2 = -0.9465$; the other half closely resembles the reflection of this half in the x-axis. Fig. 14b shows symbolically the sequence of 0's and 1's in a particular solution; the constraints evidently differ considerably from those in fig. 14a. The Lyapunov numbers are the 20th roots of those in the mapping of fig. 13, so that again $d = 1.26$. Despite the striking differences in global appearance, the local

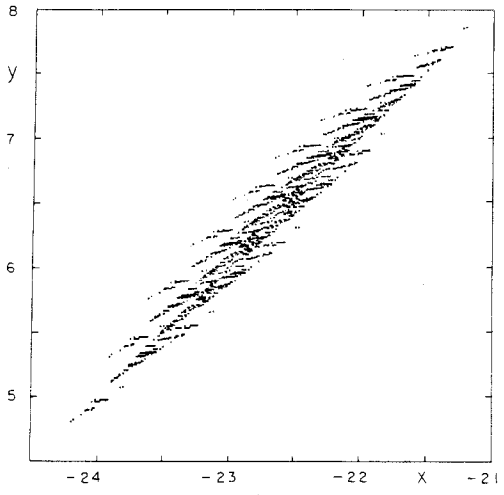

Fig. 15. The upper half of the attractor of eq. (13), when $M = 2$, $\lambda_1 = 1.0145$, and $\lambda_2 = -0.9465$. The lower half closely resembles the reflection of the upper half in the x-axis.

structures of the attractors, when viewed with sufficient magnification, appear similar.

5. Multidimensional mappings

When $M \geqq 3$, we again expect A to be the product of a continuum and a Cantor set [8, 14], but the Cantor set may be a pseudo-product. Fig. 16 shows the projections of A on the three coordinate planes, arranged as a perspective view of faces of a cube, when $M = 3$, $\lambda_1 = 5/4$, $\lambda_2 = -4/5$, and $\lambda_3 = 1/4$. The projections on the coordinate axes are similar to $R_1(4/5, S)$, $R_1(4/5, S^*)$, and $R_1(1/4, S^*)$.

Just as when $M = 2$, and for the same reasons, almost every point of A lies on a line segment contained in A, parallel to the x-axis. Likewise, the typical length of such a segment is comparable to the diameter of A, and S is again well-behaved, with $\rho(S) = \lambda_1$.

In fig. 16 we have chosen $|\lambda_2| = 1/\lambda_1$, which makes $|\lambda_2| = 1/\rho$. If S^*, like S, is well-behaved, the y-projection of A is a continuum; if S^* is ill-behaved, it is a Cantor set of capacity 1. Likewise, if S^* is well-behaved, the y–z-projection is a pseudo-product of a continuum and a Cantor set, while, if S^* is ill-behaved, it is a pseudo-product of two Cantor sets. In either case it has capacity 1.

Inspection of fig. 16 suggests that the y-projection is a continuum, implying that S^* is well-behaved, but the evidence is not conclusive; there is a suggestion of a gap near $y = 0$, which could be accompanied by narrower unresolved gaps. Fig. 17 is similar to fig. 16, with $\lambda_2 = -7/10$ instead of $-4/5$, whence $|\lambda_2| < 1/\rho$, and the y-projection is a Cantor set. The x–y- and y–z-projections are respectively a product of a continuum and a Cantor set and a pseudo-product of two Cantor sets, and in both projections the gaps in the y-values are evident. The contrast between figs. 16 and 17 lends support to the conjecture that S^* is well-behaved.

Fig. 18, which is comparable in definition to the cross section in fig. 1, shows the intersection of A with the plane $x = -1.5$, when λ_1, λ_2, and λ_3 are as in fig. 16. To construct fig. 18, we chose a point (x_0, y_0, z_0) and determined a long sequence of forward images (x_n, y_n, z_n); except for small

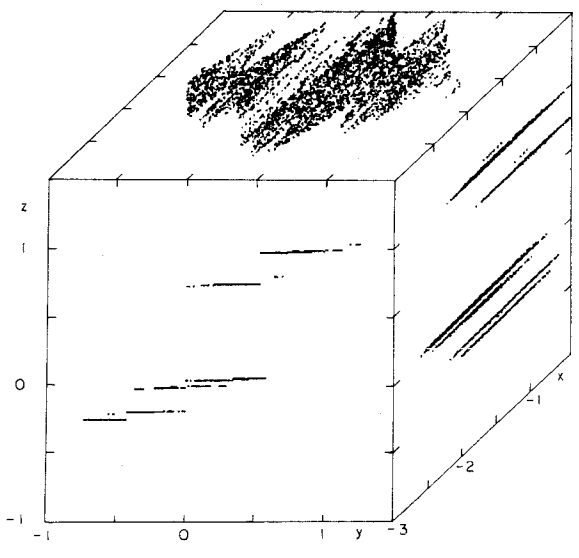

Fig. 16. The projections of the attractor of eq. (13), when $M = 3$, $\lambda_1 = 1.25$, $\lambda_2 = -0.8$, and $\lambda_3 = -0.25$, on the coordinate planes, arranged as a perspective view of faces of a cube.

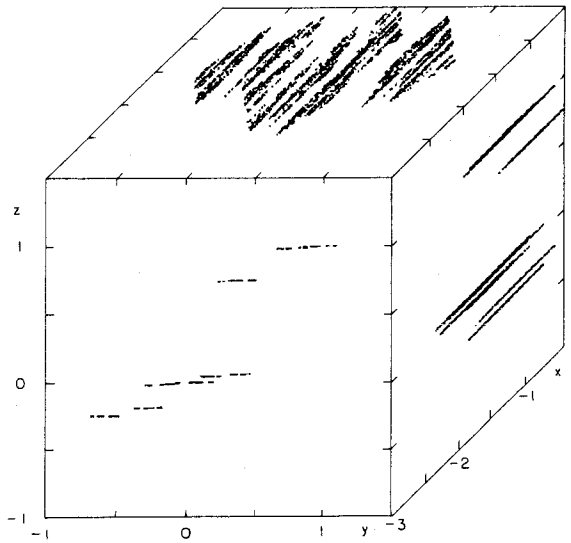

Fig. 17. Same as fig. 16, except $\lambda_1 = 1.25$, $\lambda_2 = -0.7$, and $\lambda_3 = -0.25$.

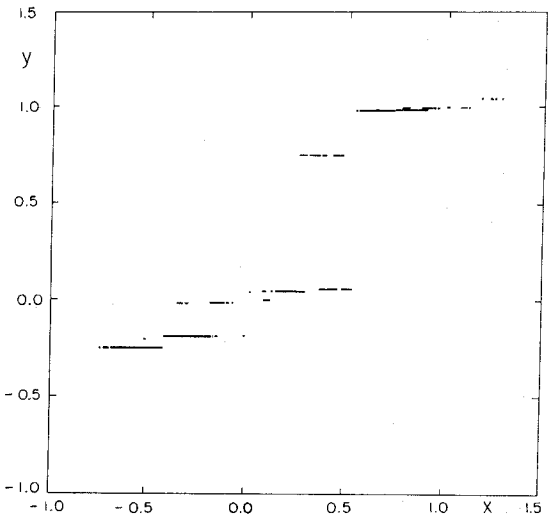

Fig. 18. The intersection of the attractor of eq. (13), when $M = 3$, $\lambda_1 = 1.25$, $\lambda_2 = -0.8$, and $\lambda_3 = -0.25$, with the plane $x = -1.5$.

values of n we assumed these to lie on A, within the limits of the round-off error. Since J_n is restricted to 0's and 1's, a point (x', y_n, z_n) lies on A if no inverse image of the segment joining it to (x_n, y_n, z_n) intersects the plane $G = 1$. We assumed that no image intersected this plane if no image of length exceeding 10^{-5} intersected the plane; this proved to be the case about two-thirds of the time. Thus the intersection of A with a surface of constant x, and the projection on a surface of constant x, have the same capacity. Whether fig. 18 shows a pseudo-product of a continuum and a Cantor set, or a pseudo-product of two Cantor sets, one with capacity 1, remains undetermined. In any event, it is not a true product of a continuum and a Cantor set; it is more like fig. 9 than fig. 13.

For a cross section where J_n is not restricted to 0's and 1's, we return to fig. 3. Again we have a pseudo-product of a continuum (presumably) and a Cantor set.

With K positive Lyapunov exponents, almost every point in A lies on a K-dimensional continuum contained in A. Thus A is the product of a K-dimensional continuum and an $(M - K)$-dimensional pseudo-product. The latter may be a pseudo-product of Cantor sets only, as in fig. 17, continua and Cantor sets, as (presumably) in figs. 3 and 16, or continua only, as for example when $M = 3$, $\lambda_1 = 1.5$, $\lambda_2 = -0.9$, and $\lambda_3 = -0.7$.

The nth forward image of a K-dimensional cube of side ε, extending in the first K directions, is a number of polyhedra whose combined volume in $(x_1, \ldots, x_K)$-space is $|\lambda_1 \cdots \lambda_K|^n \varepsilon^K$. As when $K = 1$, the number of polyhedra increases as $\rho^n(S)$, while the average volume approaches neither ∞ nor 0. Hence $\rho(S) = |\lambda_1 \cdots \lambda_K|$.

Setting $\alpha_0 = \lambda'_1 \cdots \lambda'_K$ and $\alpha_i = \lambda'_{K+i}$ in eq. (21), recalling that $\log \lambda'_i = l'_i$, and noting that the capacity of A exceeds that of the pseudo-product by K, we find that

$$d(A) = K + k + (l'_1 + \cdots + l'_{K+k})/|l'_{K+k+1}|, \tag{24}$$

where k is the largest integer making $|l'_{K+1} + \cdots + l'_{K+k}| \leqq l'_1 + \cdots + l'_K$. Setting $L = K + k$ in eq. (2), we find that $d'(A) = d(A)$.

Thus, if $\lambda_1, \ldots, \lambda_M$ are continuously varied, the integral part of d changes when $l'_1 + \cdots + l'_k = 0$ for some k. However, at least if S^* is well-behaved, the number of continua or Cantor sets involved in the $(M - K)$-dimensional pseudo-product changes when $l'_1 + \cdots + l'_K + l'_k = 0$ for some k. We conclude that transitions in the structure of the attractor need not correspond to transitions in the integral part of d.

6. Concluding remarks

We cannot claim to have employed full mathematical rigor. Our treatment of well-behaved and ill-behaved ensembles has been confined to an inspection of some simple examples; we have not shown that in general $\sigma' \leqq 1/\rho$ and $\sigma'' \geqq 1/\rho$. In describing various alternative coverings of a set by cubes, we have not eliminated the possibility of some still more efficient coverings. We have used a special definition of attractors in order to establish that some of the apparent line segments are true line segments, and we have not shown that this

definition does not introduce some unwanted features. In any event, our conclusions are based upon a special system of equations.

The question arises as to whether the attractors of more general mappings or flows have similar local structures, or whether the present structures have somehow been produced by the broken linearity. Our original conclusion concerning fig. 1, for example, was that it appeared to be locally the product of a continuum and a Cantor set. The present study suggests that it may be a pseudo-product, since the two associated Lyapunov exponents are both negative. Our former conclusion was based largely on the discovery that, within the limits of numerical precision, an arbitrary line segment cutting across the apparent continua would intersect these in an infinite complex of points. We have seen that the same thing can happen in a pseudo-product.

This situation illustrates the difficulties which may be encountered in drawing conclusions from numerical output, even with fairly high precision, and the even greater difficulties in drawing conclusions from graphical displays. In fig. 9, for example, it might not be apparent from ordinary double-precision computations that a horizontal line can be drawn between any two points of the set. In fig. 1, the analogues of these horizontal lines, if they exist, would be difficult to identify, since the procedures which we have so far discovered for examining the system are numerical. However, numerical and even graphical results may lead to hypotheses which can subsequently be verified by other means; they may also be effective in disproving some unverified conjectures.

A number of writers have viewed with disfavor the term "strange attractor" to describe an attractor whose structure involves Cantor sets. Chirikov and Izrailev [15] state that "[a strange] attractor seems strange only for a stranger". Their point is that the presence of Cantor sets should have been anticipated. The existence of mappings where the coordinates of a point on an attractor are expressible as power series, whose coefficients are bounded and whose arguments are Lyapunov numbers, would appear to support their statement.

Acknowledgements

Most of this research was supported by the GARP Program of the Atmospheric Sciences Section, National Science Foundation, under Grant 82-14582 ATM. Part of the work was performed while the author was a summer visitor at the National Center for Atmospheric Research, Boulder, Colorado; NCAR is supported by the National Science Foundation.

References

[1] M. Hénon, Comm. Math. Phys. 50 (1976) 69.
[2] J. Guckenheimer and P. Holmes, Nonlinear Oscillations, Dynamical Systems, and Bifurcations of Vector Fields (Springer, New York, 1983) pp. 36, 256.
[3] D. Ruelle, Comm. Math. Phys. 82 (1981) 137.
[4] C. Conley, CBMS Regional Conferences in Mathematics 38, (Am. Math. Soc., Providence, 1978).
[5] J.D. Farmer, E. Ott and J.A. Yorke, Physica 7D (1983) 153.
[6] J. Kaplan and J.A. Yorke, Lecture Notes in Mathematics 730 (Springer, Berlin, 1978) 228.
[7] E.N. Lorenz, Physica 8D (1984) 90.
[8] S. Smale, Bull. Amer. Math. Soc. 73 (1969) 747.
[9] R.F. Williams, Ann. of Math. 98 (1973) 120, 99 (1974) 380.
[10] R. Bowen and J.M. Franks, Ann. of Math. 106 (1977) 73.
[11] J.M. Franks, CBMS Regional Conference in Mathematics 49 (Am. Math. Soc., Providence, 1982).
[12] R. Bowen and O. Lanford, Proc. Sympos. Pure Math. 14 (Am. Math Soc., Providence, 1970) p. 23.
[13] J. Alexander and J.A. Yorke, Ergod. Th. and Dynam. Syst. 4 (1984) 1.
[14] R.F. Williams, Pub. Math. I.H.E.S. 43 (1973) 169.
[15] B.V. Chirikov and F.M. Izrailev, Institute of Nuclear Physics, Novosibirsk (1979) preprint.